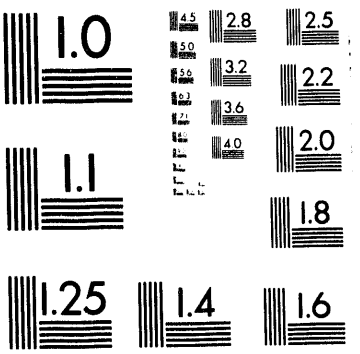
1.0
1.1
1.25
1.4
1.6
1.8
2.0
2.2
2.5
2.8
3.2
3.6
4.0
4.5
5.0
5.6
6.3
7.1
8.0
9.0

1 of 1

Conf-9309300--1

UCRL-JC-115337
PREPRINT

Carbon Cycle Modeling Calculations for the IPCC

D. J. Wuebbles
A.K. Jain

This paper was prepared for submittal to the
IPCC Working Group 1 Meeting
Carqueiranne, France
September 18, 1993

August 12, 1993

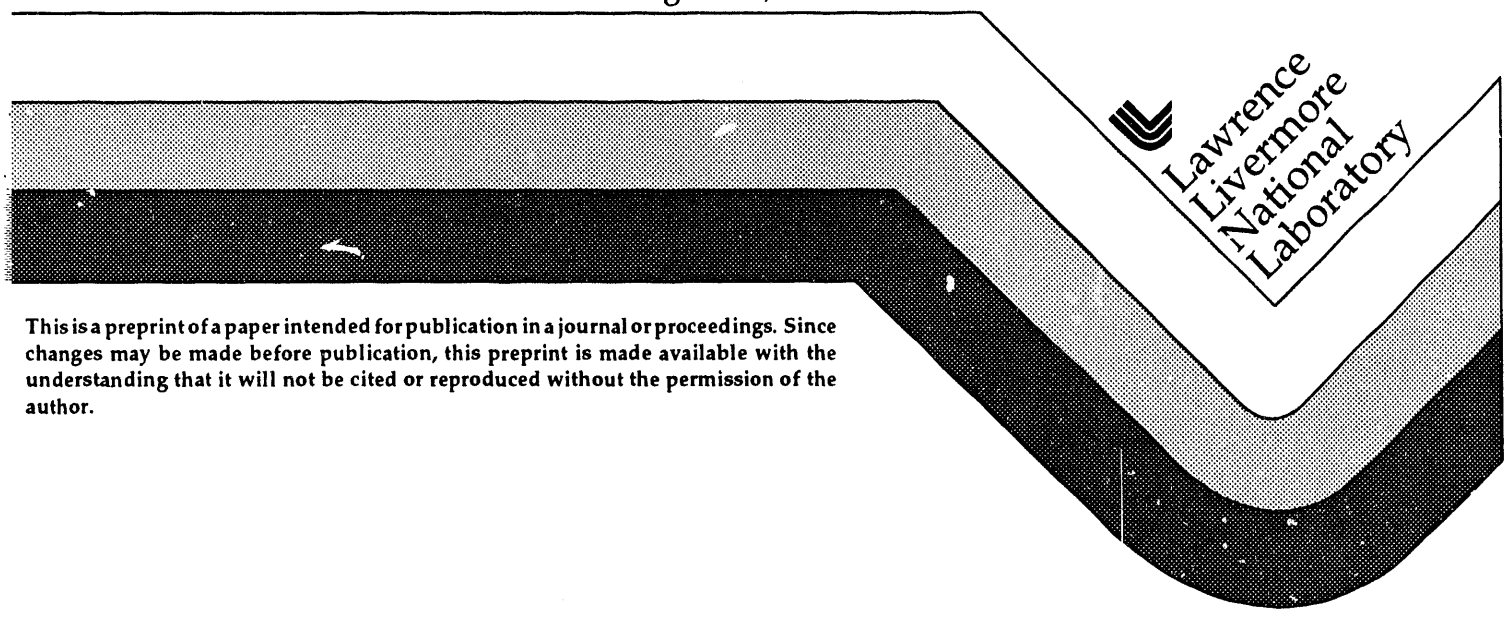

Carbon Cycle Modeling Calculations for the IPCC

by
Donald J. Wuebbles and Atul K. Jain
Global Climate Research Division
Lawrence Livermore National Laboratory
Livermore, CA 94550

Introduction

We have carried out essentially all the carbon cycle modeling calculations that were required by the IPCC Working Group 1. Specifically, IPCC required two types of calculations, namely, 'inverse calculations' (input was CO_2 concentrations and the output was CO_2 emissions), and the 'forward calculations' (input was CO_2 emissions and output was CO_2 concentrations). In particular, we have derived carbon dioxide concentrations and/or emissions for the following scenarios using our coupled climate-carbon cycle modelling system:

Inverse Calculations

Stabilization scenarios: S350, S450, S550, S650, and S750 (Figs. 1a–d)
Delayed scenarios: DS450 and DS550 (Figs. 1a–d)

Forward calculations

IPCC emission scenarios: IS92a, IS92b, IS92c, IS92d, IS92e, and IS92f (Fig.2)
The science scenarios: DEC0%, DEC1%, and DEC2% (Fig.3)

Impulse response function

Iinit case (10 Gt C pulse release in pre-industrial atmosphere) (Fig.4)
Iper case(10 Gt C pulse release in 1995 atmosphere) (Fig.4)

^{14}C calculations

Mixed layer ^{14}C ratios from 1800 to 1990 (Fig.5)
Ocean ^{14}C inventory for year 1974 (see text)

In the following we briefly describe our model and some of the main features of our model calculations.

The Carbon Cycle Model

A newly developed globally averaged carbon cycle model has been used to estimate emissions and concentrations of CO_2 for required IPCC scenarios. The model consists of four reservoirs: atmosphere, biosphere, mixed layer of the ocean, and the deep ocean. The atmosphere and mixed layers are considered as well-mixed reservoirs. However, the deep ocean is treated as advective-diffusive medium with a continuous distribution of total inorganic carbon as described by one-dimensional conservation-of mass equation (Hoffert et al., 1981). The upwelling diffusion (UD) ocean includes the polar sea box which closes the thermohaline

This work was performed under the auspices of the U.S. Department of Energy by the Lawrence Livermore National Laboratory under Contract No. W-7405-Eng-48.

circulation. In our UD model the physical transport processes are characterized by eddy diffusivity K and upwelling velocity w. To the model deep ocean an additional carbon source term is added that is associated with the oxidation of the organic debris containing the carbon removed in the mixed layer by photosynthesis. The dynamic ocean model parameters - the eddy diffusivity K, upwelling velocity w, and atmosphere-ocean exchange coefficient, k_{am} (or the corresponding gas exchange rate) - are determined by the calibration method based on matching the natural as well as bomb-produced ^{14}C. The estimated values of K, w and k_{am} are 4700 m^2/yr, 3.5 m/yr, and 0.13 per yr (or the corresponding gas exchange rate 17.8 mol/m^2/yr), respectively (Table 1).

The ocean buffer factor that summarizes the chemical re-equilibration of sea water with respect to CO_2 variations is calculated from the set of chemical equations of borate, silicate, phosphate, and carbonate chemistry and the temperature-dependent rate constants as given by Peng et al.(1987).

There is an important feedback for the atmospheric CO_2, namely, the direct interaction of atmospheric CO_2 with the deep ocean which is nearly free of excess CO_2. We have taken this feedback into account by introducing a polar sea feedback parameter, π_c, defined as the change in the surface concentration in the polar region relative to that in the non-polar region. This parameter is similar to that used by IPCC in their energy balance model to represent the variation of polar sea temperature. The value of π_c would lie between 0.0 and 1.0. For $\pi c = 0.4$, the model estimated average CO_2 uptake rate for the period 1980–1989 is 2.1 GtC/yr which is in good agreement with the IPCC estimates of 2.0±0.8 GtC/yr. Therefore, we have used $\pi_c = 0.4$ in our model calculations.

For estimating the terrestrial biospheric fluxes, a six-box globally aggregated terrestrial biosphere submodel coupled to the atmosphere box has been used. The six boxes are ground vegetation, non woody tree parts, woody tree parts, detritus, mobile soil (turn over time 75 years), resistant soil (turnover time 500 years). The model equations that describe the rate of change of carbon in each boxes are those taken from Harvey(1989). The photosynthesis rate in the submodel is simulated by increasing carbon dioxide concentrations in the atmosphere by logarithmic law and a fertilization factor $\beta = 0.42$. The flow coefficients are temperature dependent according to an Arrhenius law. A one-dimensional upwelling-diffusion model of Harvey and Schneider (1985) is used to infer the surface temperature change and oceanic uptake of heat.

Inverse Calculation

For the inverse calculations we have solved the following balance equation

$$E_{tot} = 2.123\ N_a + F_{oc}$$

where net total emission E_{tot} is the sum of industrial emission (E_{in}), land use emissions (E_{ln}) and a miscellaneous sink (E_{bs}). F_{oc} is the ocean flux. The factor 2.123 converts 1 ppmv of CO_2 into GtC. In our calculations, we assume that the miscellaneous sink is represented by the biospheric sink through an enhancement of vegetation growth. Thus the net biospheric flux $F_{nb} = F_{ln} - E_{bs}$. The term F_{oc} is calculated from the prescribed observed atmospheric CO_2 concentration N_a. The net biospheric flux (F_{nb}) is calculated by subtracting well-known industrial emissions (E_{in}) from the net total emission (E_{tot}). Fig. 6 shows the model estimated CO_2 fluxes from 1765 to 1990 for the inverse calculation.

Net Land Use Emissions

Our major uncertainties about the CO_2 sinks arise from the lack of direct measurements of terrestrial biospheric fluxes. The estimates of biotic emissions of the time course differ widely. Studies on isotopes show a maximum biotic CO_2 release in the late 19th or early 20th century with a progressive reduction thereafter. In contrast, a study based on ecological reconstruction show a generally increasing rate of release reaching a maximum between 1950 and 1980 (although less steep than of the fossil CO_2) (Houghton, 1991). Recent estimates of the release of carbon from terrestrial ecosystems as a result of deforestation and reforestation, for year 1990, range between 1.5 and 2.7 GtC (Houghton, 1991) which are about 50% higher than those in 1980. The net release of carbon from changes in land use worldwide is inconsistent with the results of geochemical models of the carbon cycle. Therefore, the modelers have had to rely on model parameterizations to estimate the emission of CO_2 from deforestation and land use. The net land use emissions in our calculations are derived by means of an inverse method. Usually the input to the terrestrial biosphere submodel is net land use emissions and the output is net biospheric fluxes. We run the biosphere submodel in an inverse mode using the net biospheric flux (F_{nb}) as input and obtain the net land use emissions. For consistency, we run the model in normal model using the net land use emissions as input. Fig. 7 clearly indicates that the net biospheric fluxes are remarkably similar in both modes. IPCC supplied net biospheric emissions are also shown in the figure for comparison that are based on changes in land use. The IPCC estimates indicate a continuous increasing trend during 1765 to 1990. In contrast to IPCC estimates, our model results show an increasing trend in the 19th century and beginning with 1900 a slow decrease and then rapid increase starting in the late 1970s. These trends are consistent with the isotopic measurement. For period 1980 to 1989, our model estimated emissions from land use of 1.6 GtC/yr are in agreement with the IPCC estimate of 1.6 ± 1.0 GtC/yr. The model derived value for 1990 was 1.7 GtC.

Impulse Response Curves

Fig. 4 shows the impulse response curves derived for the requested cases. For all the cases the pulse is 10 Gt C as proposed by IPCC. However, the time of the pulse given is different for both the cases. In the 'equilibrium case' the pulse is instantaneously injected into the steady state atmosphere. In the 'perturbation case' the model was initialized to a 278 ppmv steady-state at year 1765. The ocean model was then run from 1765 to 1990, with the specified total CO_2 emissions as obtained from the inverse calculations. From 1990 onwards, the model was run with the S650 emission scenario both with and without an additional 10 Gt C pulse injected into the 1995 atmosphere. It is interesting to note that the impulse response function is sensitive to the initial state of the ocean-atmosphere system into which CO_2 is emitted. This is due to the fact that in our model the CO_2 flux from the atmosphere to the mixed layer is a nonlinear function of ocean surface total carbon which appears in the buffer factor ξ. At the pre industrial time, short term CO_2 absorption capacity of ocean was higher. Therefore in the first fifty years the decay of the CO_2 was more rapid in the equilibrium case than in the perturbation case. When the industrial production continues to increase, ξ will rise with the partial pressure of CO_2 in the mixed layer. At the same time the short term capability of the oceans to absorb CO_2 from the atmosphere will decrease. Fig. 4 also shows that the response functions for both cases (perturbation and equilibrium cases) are similar when ξ remains constant with time.

Bomb ^{14}C Inventories

The average oceanic inventory of bomb–^{14}C is determined by integrating the difference between the pre-bomb (1950) and post-bomb (1974) vertical profiles. An average model estimated total CO_2 concentration of 2.31 mol/m^3 is used to convert model ^{14}C units into ^{14}C inventories. The model estimated bomb–^{14}C and the penetration depth are $8{\cdot}4 \times 10^{13}$ atom/m^2 and 310 m, respectively.

Major Findings

The model described here to account for CO_2 and exchange with the deeper regions of the world ocean has been calibrated using the distributions of natural as well as of bomb-produced ^{14}C. It is based on an admittedly simplified view of large-scale thermohaline circulation leading to a world ocean depicted as an upwelling-diffusion 1-D model with recirculation of polar bottom water in a polar sea. Despite its simplicity, the model is able to consistently simulate different phenomena of the global carbon cycle, in particular the steady state ^{14}C (Fig. 8) and inorganic carbon (Fig. 9) distribution in the deep ocean, the anthropogenic CO_2 increase, and the corresponding CO_2 dilution effect (Suess effect) (Fig. 5) as well as bomb produced ^{14}C distribution in the ocean (Fig. 10). Finally, the biospheric component of the model is also able to predict the emissions due to land use changes and net biospheric fluxes (Fig. 7).

Acknowledgments

Work performed under the auspices of the U.S. Department of Energy at Lawrence Livermore National Laboratory under Contract W-7405-ENG-48. We thank M.I. Hoffert for helpful comments.

References

Harvey, L. D. D., and S. H. Schneider (1985): Transient climate response to external forcing on 10^0–10^4 year time scales, Part 1: Experiments with globally averaged, coupled, atmosphere and ocean energy balance models, J. Geophys. Res., 90, 2191–2205.

Harvey, L. D. D.(1989): Managing Atmospheric CO_2, Clim. Change, 15, 343–381.

Hoffert, M. I., A. J. Callegari, and C. T. Hseis (1981): A box diffusion carbon cycle model with upwelling, polar bottom water formation and a marine biosphere, in Carbon Cycle Modelling, SCOPE 16, edited by B. Bolin, 287–305, John Wiley, New York.

Houghton, R. A. (1991): Tropical deforestation and atmospheric carbon dioxide, Climatic Change, 19, 99–118

Peng, T. H., T. Takahashi, W. S. Broecker, and J. Olafasson (1987): Seasonal variability of carbon dioxide, nutrients and oxygen in the northern North Atlantic surface water, Tellus, 39B, 439–458.

Siegenthaler, U., and F. Joos (1992): Use of a simple model for studying organic tracer distributions and a global carbon cycle, Tellus, 44B, 186–207.

Figure Captions

Figure 1: Model estimated changes in (a) total CO_2 emissions (b) Net biospheric fluxes (c) fossil fuel emissions and (d) ocean fluxes for stabilization scenarios S350-750 and delayed scenarios DS450 and DS550 for the period 1990 to 2300.

Figure 2: Model estimated concentrations of CO_2 from 1990 to 2100 for the IPCC emission scenarios IS92a-f.

Figure 3: Model estimated concentrations of CO_2 from 1990 to 2100 for the science scenarios DEC0% , DEC1%, and DEC2%.

Figure 4: Model response of atmospheric CO_2 to a pulse of 10 GtC for the Perturbation (Ipert) and the Equilibrium (Iinit) cases. In the Iint case, pulse is released in pre-industrial atmosphere and in the perturbation case, pulse is released in 1995 atmosphere.

Figure 5: Model estimated ^{14}C concentration (‰) in mixed layer from 1800 to 1990. These concentrations are calculated from the observed atmospheric ^{14}C concentration date also shown in the figure. The atmospheric values are the average values of the northern (extra tropical), southern (extra tropical) and equatorial regions as compiled by M. Heimann for IPCC.

Figure 6: Result from the inverse calculation by using the CO_2 concentration history as an input from 1765 to 1990. The calculations yield the total CO_2 emissions. The net biospheric fluxes are estimated by subtracting the fossil emissions from the total emissions.

Figure 7: Model estimated annual net land use emissions and net biospheric fluxes for the period 1765–1990. The figure also shows the comparison of the modeled with the observed emissions from IPCC.

Figure 8: Comparison of the model estimated steady-state ^{14}C (‰) in the deep ocean with the observed data. The observed estimated values are taken from Siegenthaler and Joos(1992)

Figure 9: Comparison of the model estimated steady-state total inorganic carbon (mole/m^3)with the observed data in the deep ocean. The observed data is the globally averaged data estimated from the GEOSECS data (Takahashi et al., 1981).

Figure 10: Comparison of the model estimated bomb-produced ^{14}C (‰) in the deep ocean with the observed data. The observed values, estimated from the GEOSECS data, are taken from Siegenthaler and Joos(1992).

Table 1 Values of the parameters for the carbon cycle model

CO_2 concentration in pre-industrial atmosphere	278 ppm
CO_2 mass in pre-industrial atmosphere	590 Gt C
CO_2 mass in pre-industrial mixed layer	676 GT C
Carbon concentration in pre-industrial mixed layer	2.05 mol m^{-3}
Carbon concentration in the pre-industrial polar sea	2.37 mol m^{-3}
CO_2 biospheric mass in pre-industrial ocean	2327 Gt C
^{14}C concentration in pre-industrial atmosphere	1 (0‰)
^{14}C concentration in pre-industrial mixed layer	0.95 (-50 ‰)
^{14}C concentration in pre-industrial polar sea	0.85 (-150‰)
Average ^{14}C concentration in pre-industrial ocean below 75 m	0.84 (-160 ‰)
Average depth of the mixed layer	75m
Average depth of the deep ocean	4000m
Ocean surface area	$3.62\times10^{14}m^2$
Eddy diffusivity K	4700 m^2 yr^{-1}
Upwelling velocity w	3.5 m yr^{-1}
Gas exchange rate at 278 ppmv	14.9 (mol m^2 yr^{-1})
Buffer factor for excess CO_2	see text
Decay constant of ^{14}C	1/8267 yr
Fertilization Factor β	0.42
Bottom water surface concentration feedback parameter Πc	0.4

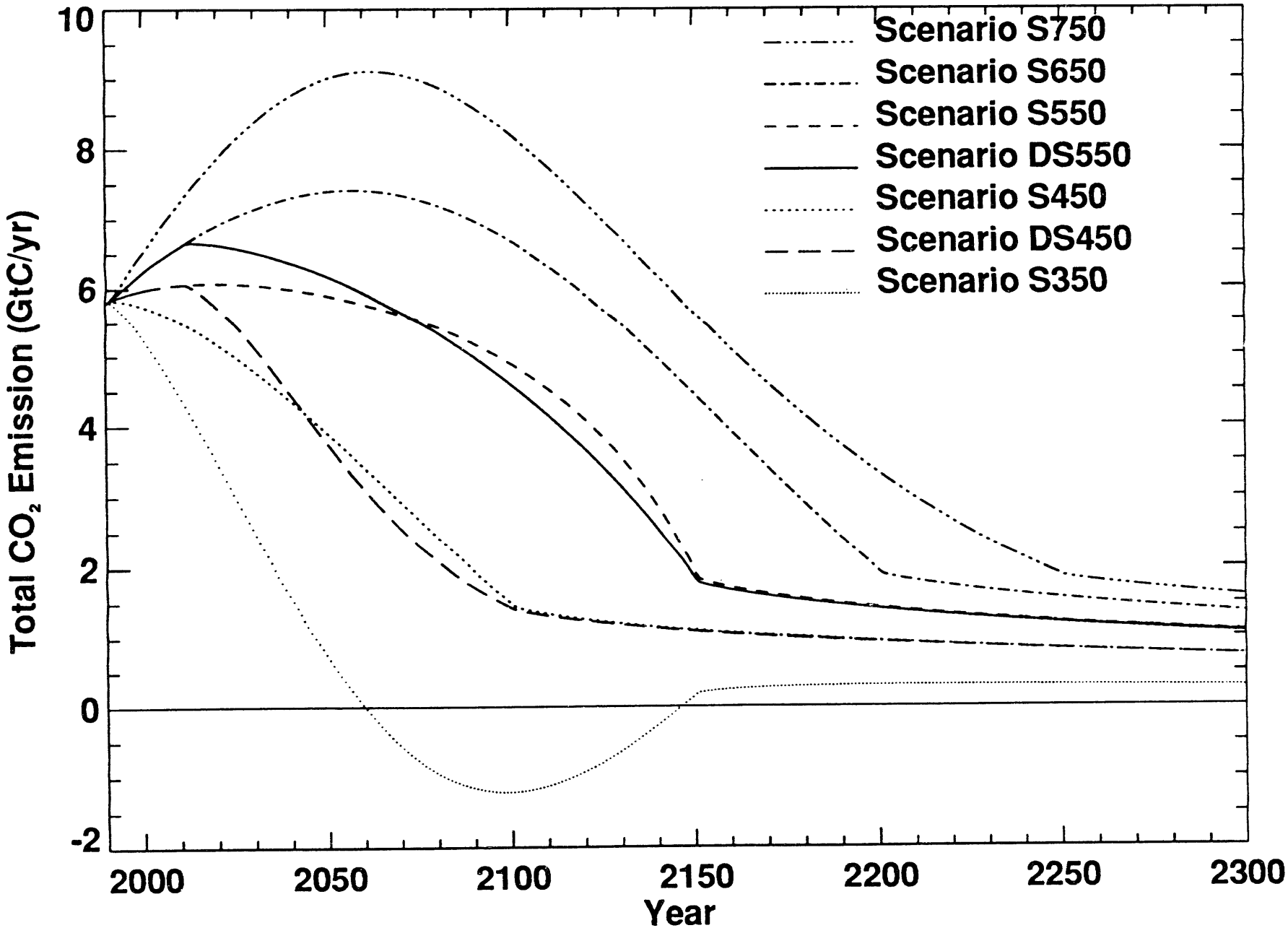
Scenario S750
Scenario S650
Scenario S550
Scenario DS550
Scenario S450
Scenario DS450
Scenario S350
Total CO_2 Emission (GtC/yr)
10
8
6
4
2
0
-2
2000
2050
2100
2150
2200
2250
2300
Year

Figure 1A

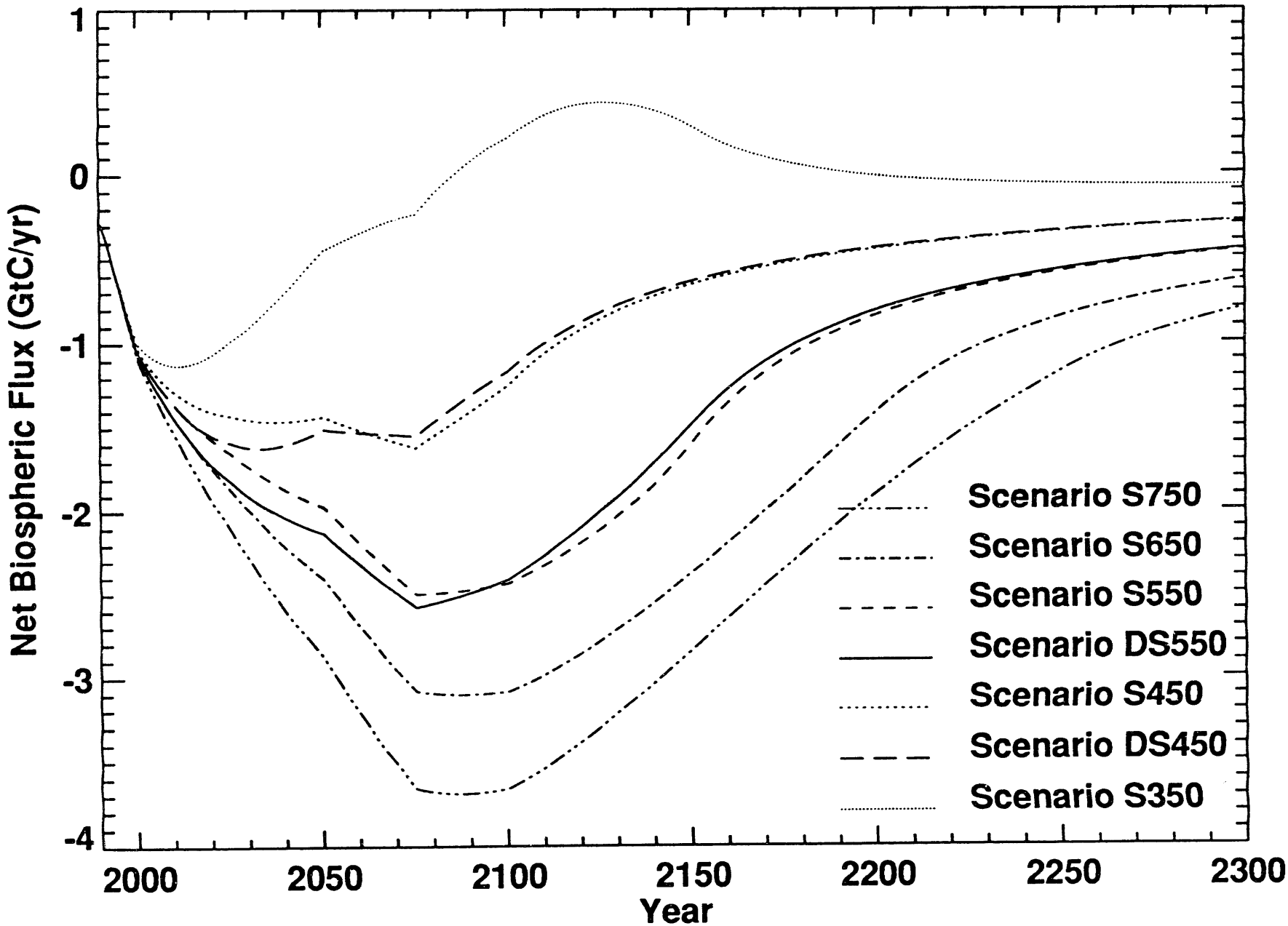
Net Biospheric Flux (GtC/yr)
1
0
-1
-2
-3
-4
2000
2050
2100
2150
2200
2250
2300
Year
Scenario S750
Scenario S650
Scenario S550
Scenario DS550
Scenario S450
Scenario DS450
Scenario S350

Figure 1B

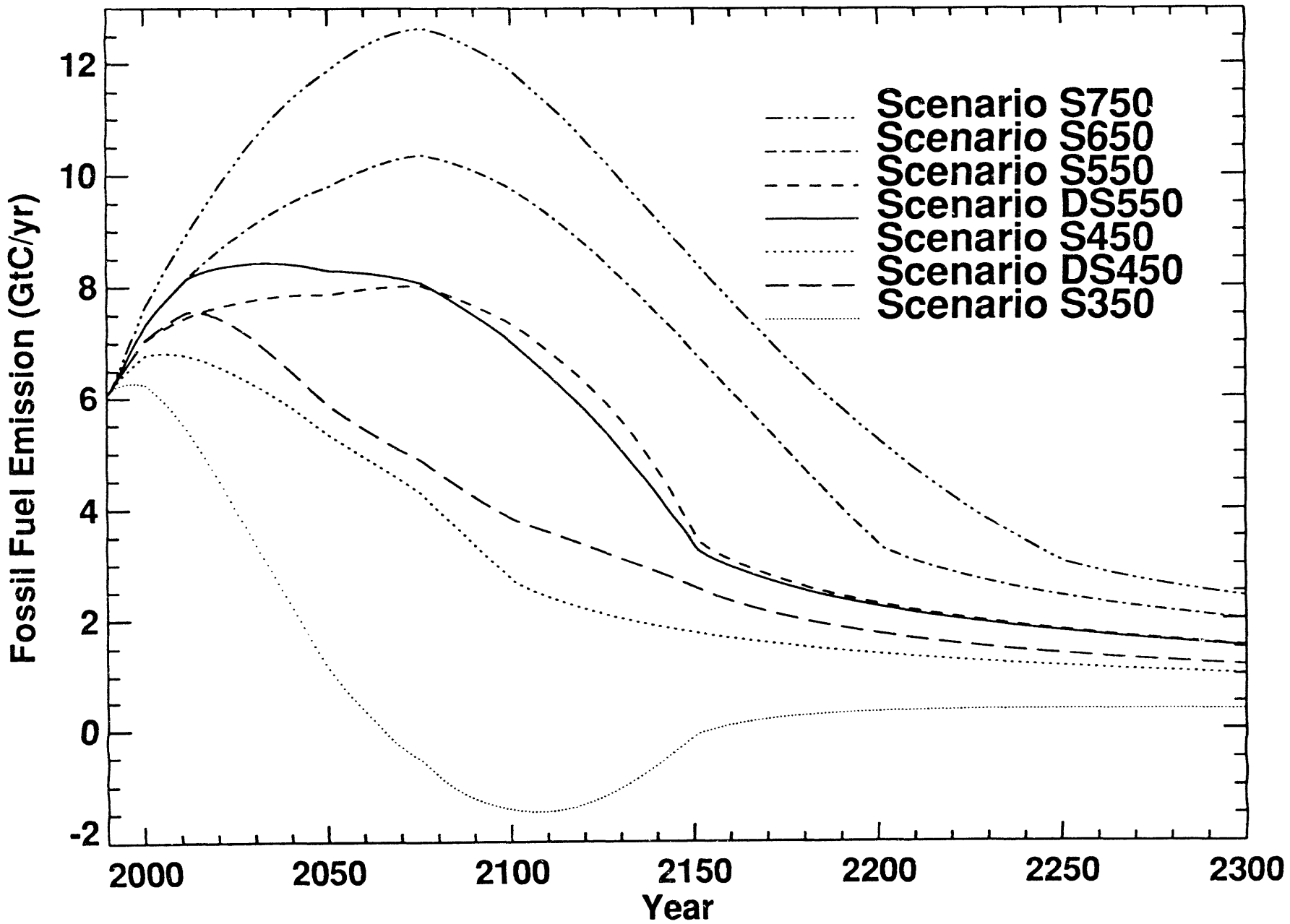
Fossil Fuel Emission (GtC/yr)
12
10
8
6
4
2
0
-2
2000
2050
2100
2150
2200
2250
2300
Year
Scenario S750
Scenario S650
Scenario S550
Scenario DS550
Scenario S450
Scenario DS450
Scenario S350

Figure 1C

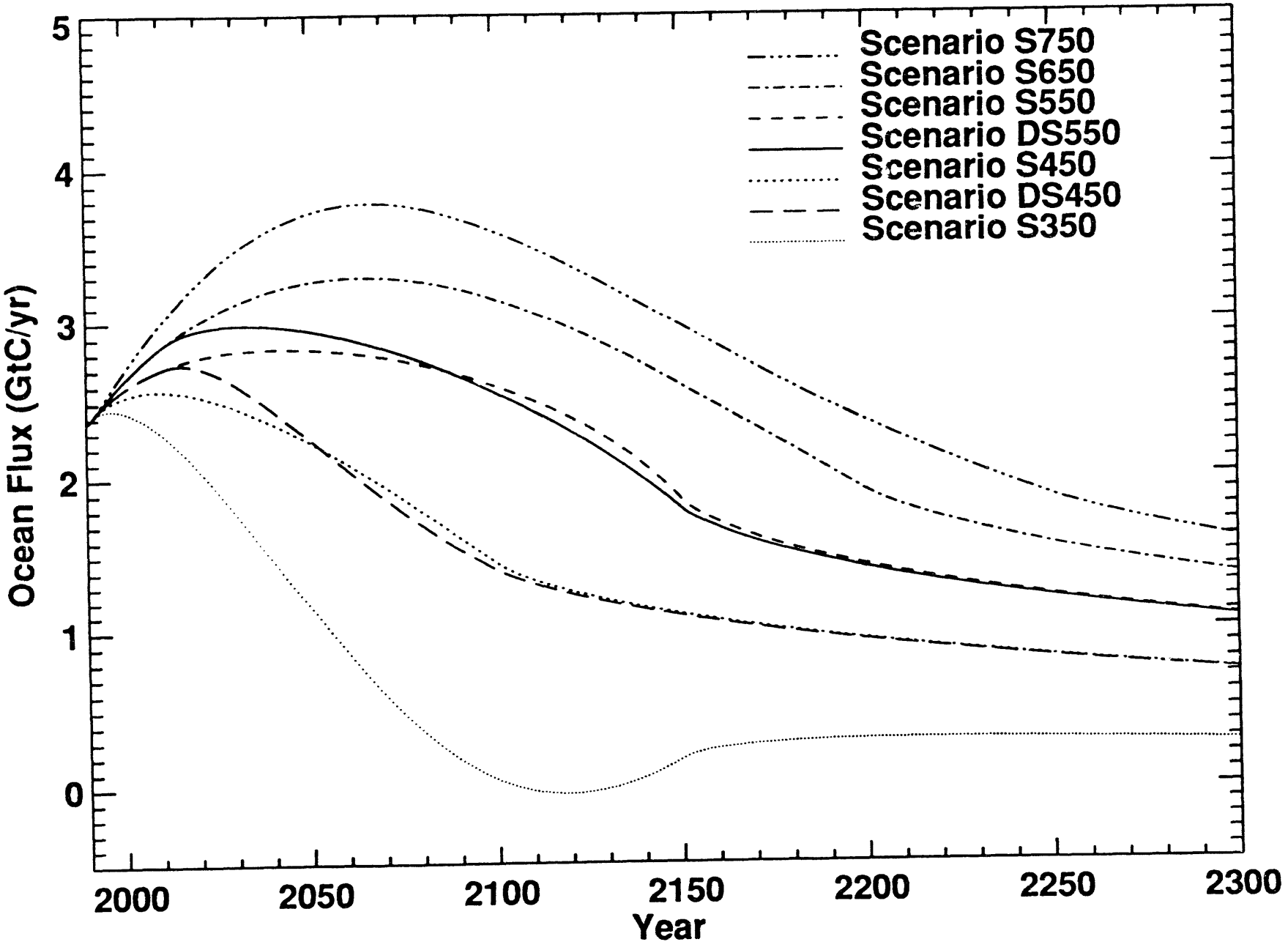
Scenario S750
Scenario S650
Scenario S550
Scenario DS550
Scenario S450
Scenario DS450
Scenario S350
Ocean Flux (GtC/yr)
5
4
3
2
1
0
2000
2050
2100
2150
2200
2250
2300
Year

Figure 1D

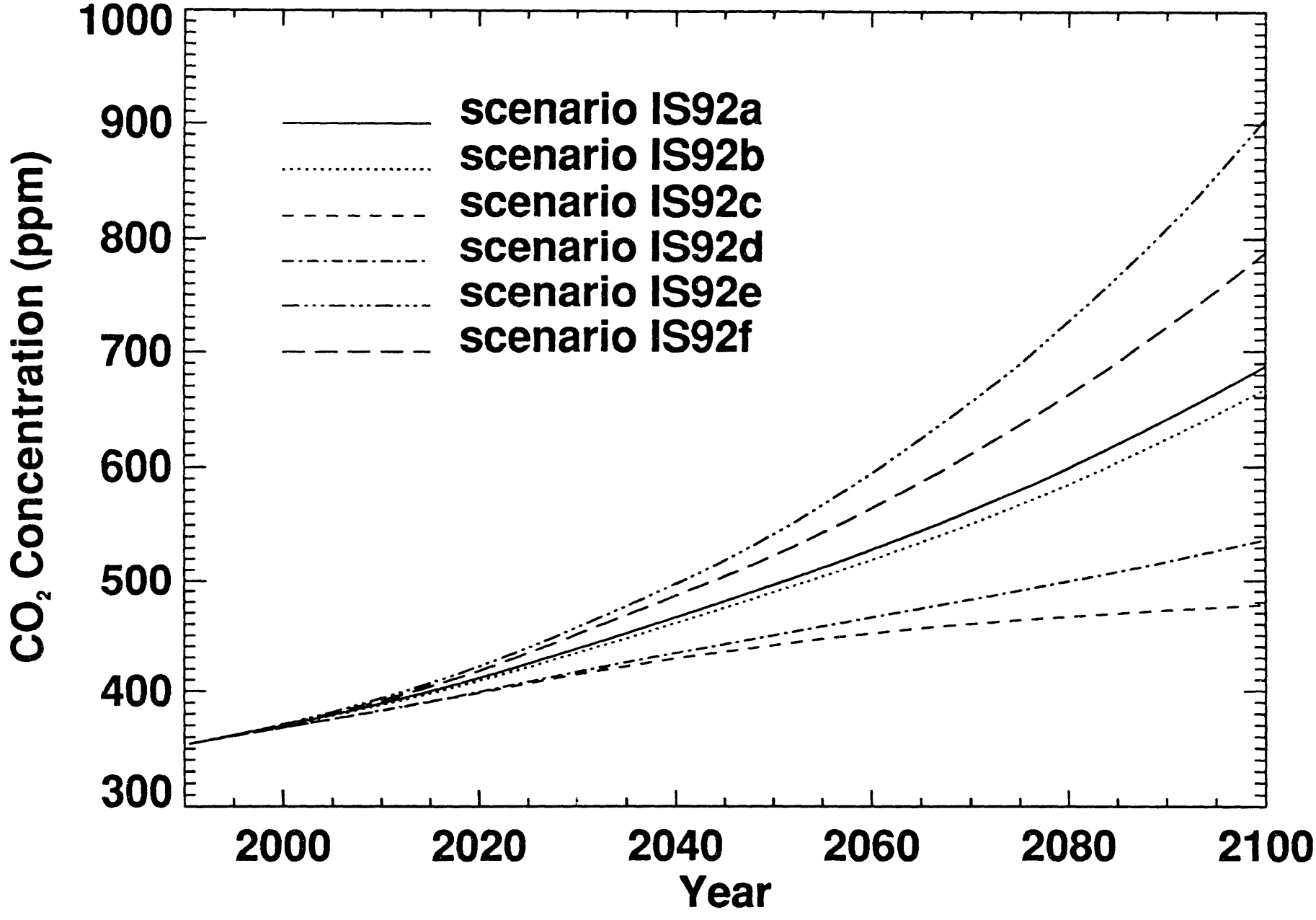
1000
900
800
700
600
500
400
300
CO_2 Concentration (ppm)
scenario IS92a
scenario IS92b
scenario IS92c
scenario IS92d
scenario IS92e
scenario IS92f
2000
2020
2040
2060
2080
2100
Year

Figure 2

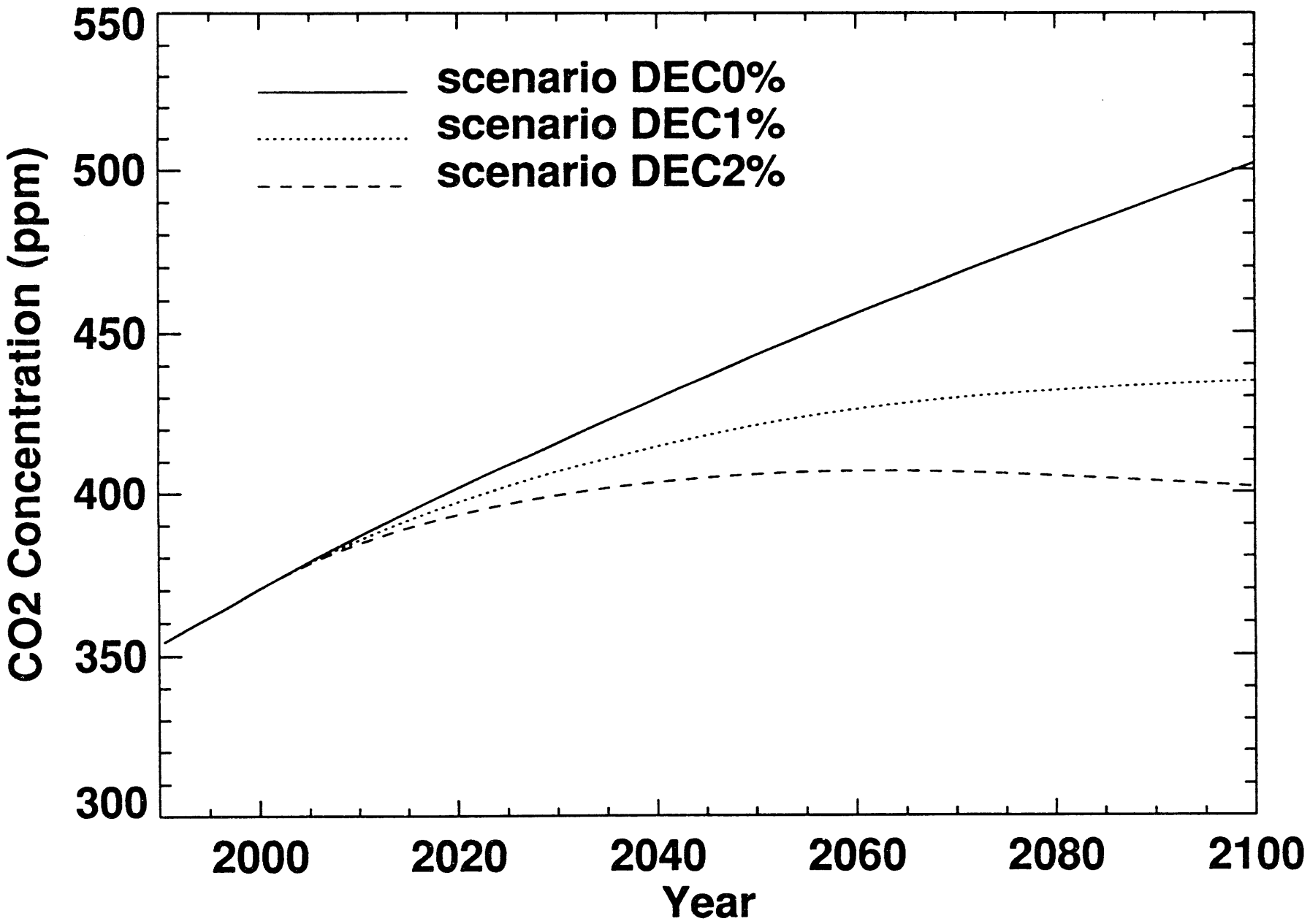
scenario DEC0%
scenario DEC1%
scenario DEC2%
CO2 Concentration (ppm)
550
500
450
400
350
300
2000
2020
2040
2060
2080
2100
Year

Figure 3

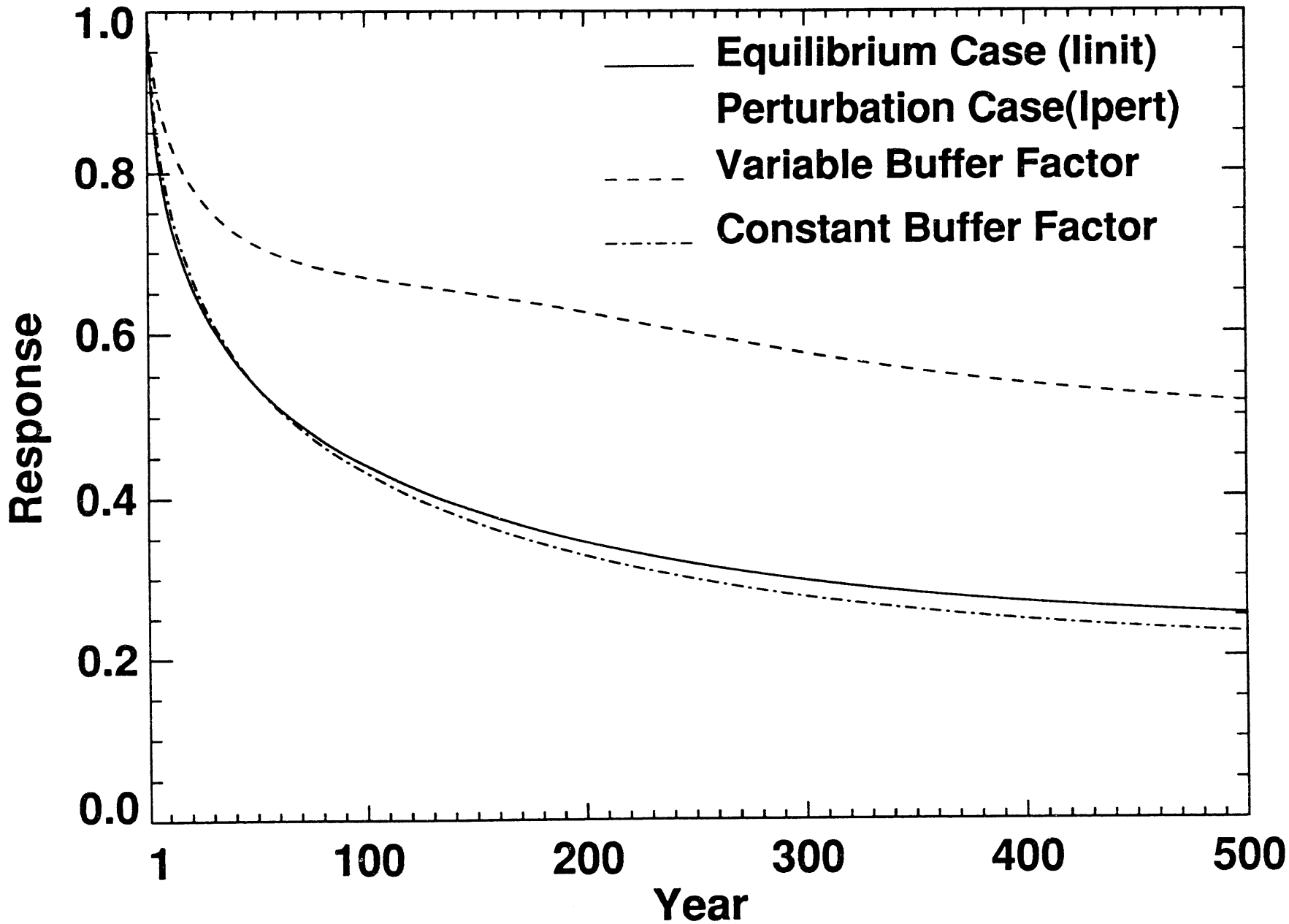
Equilibrium Case (Iinit)
Perturbation Case(Ipert)
Variable Buffer Factor
Constant Buffer Factor
Response
1.0
0.8
0.6
0.4
0.2
0.0
1
100
200
300
400
500
Year

Figure 4

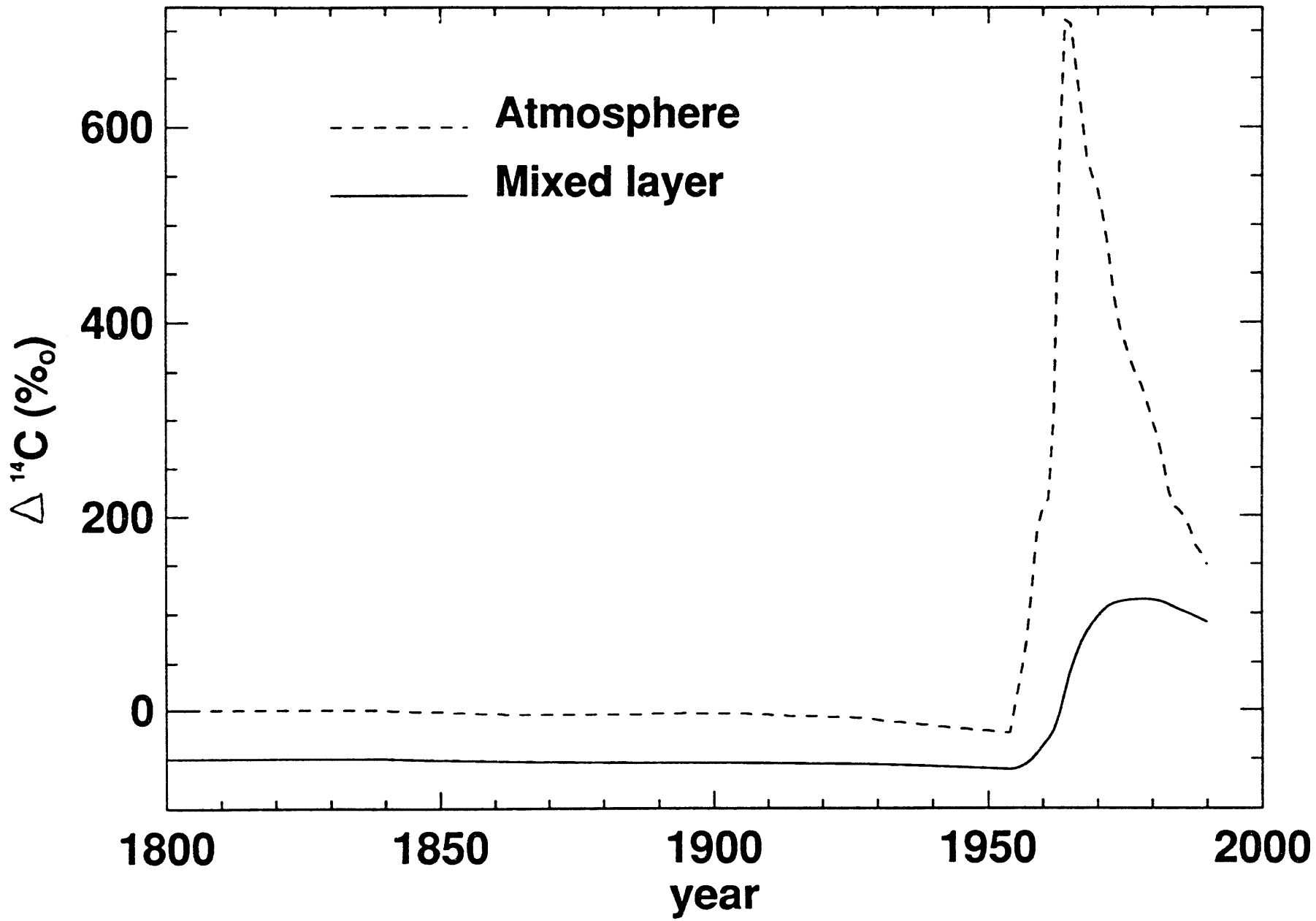
Atmosphere
Mixed layer
600
400
200
0
Δ 14C (‰)
1800
1850
1900
1950
2000
year

Figure 5

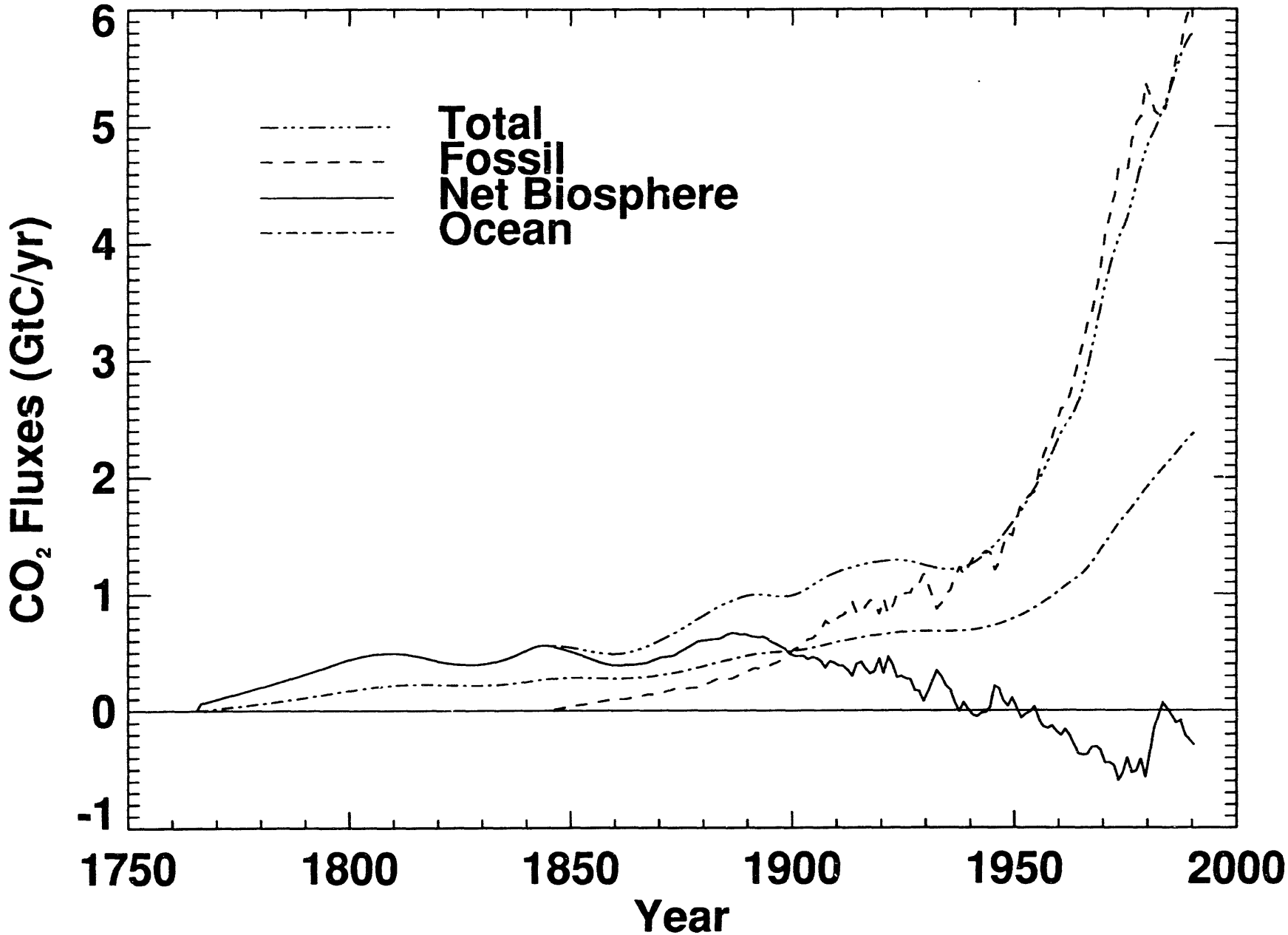
Total
Fossil
Net Biosphere
Ocean
CO_2 Fluxes (GtC/yr)
6
5
4
3
2
1
0
-1
1750
1800
1850
1900
1950
2000
Year

Figure 6

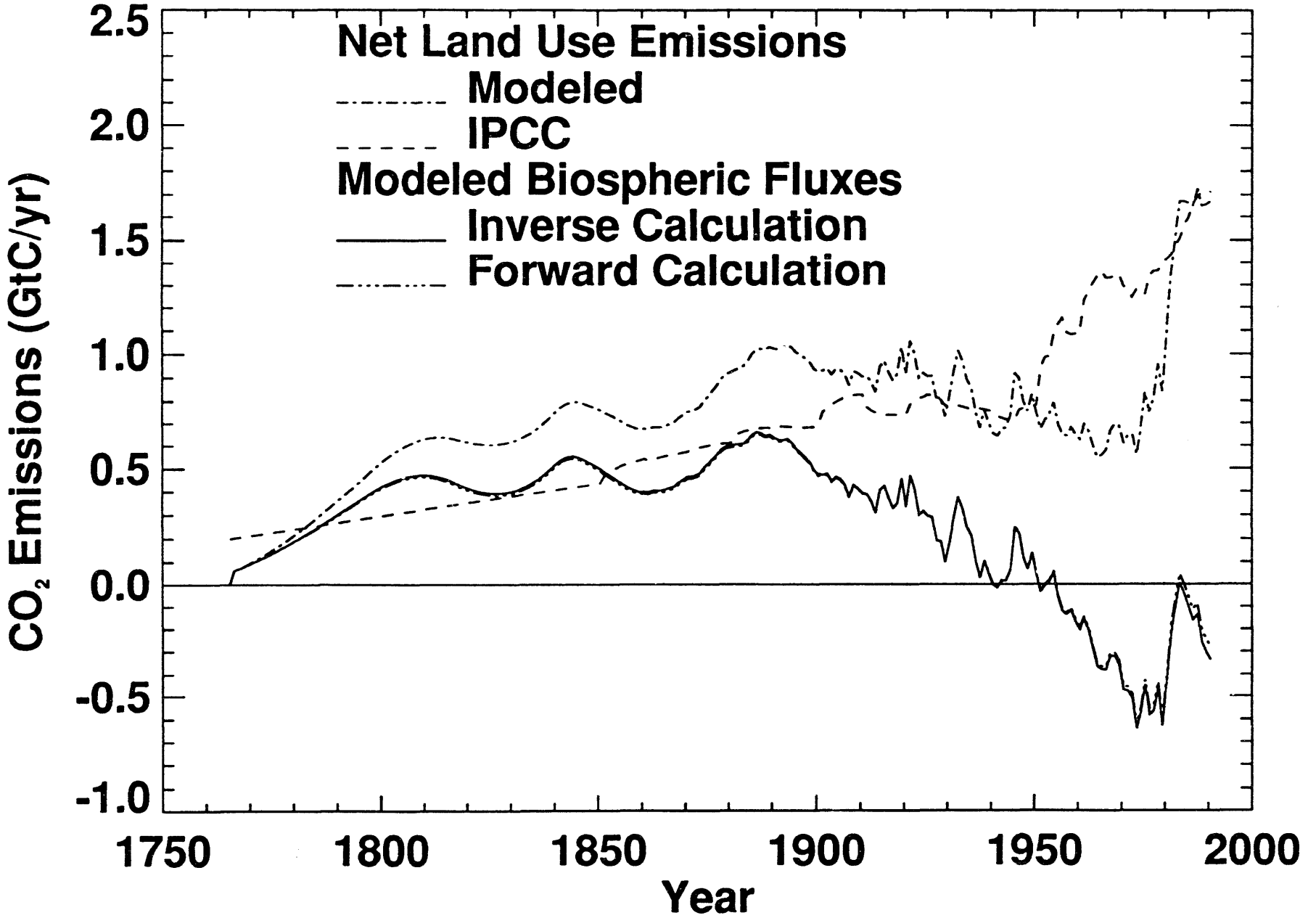
Net Land Use Emissions
Modeled
IPCC
Modeled Biospheric Fluxes
Inverse Calculation
Forward Calculation
CO_2 Emissions (GtC/yr)
2.5
2.0
1.5
1.0
0.5
0.0
-0.5
-1.0
1750
1800
1850
1900
1950
2000
Year

Figure 7

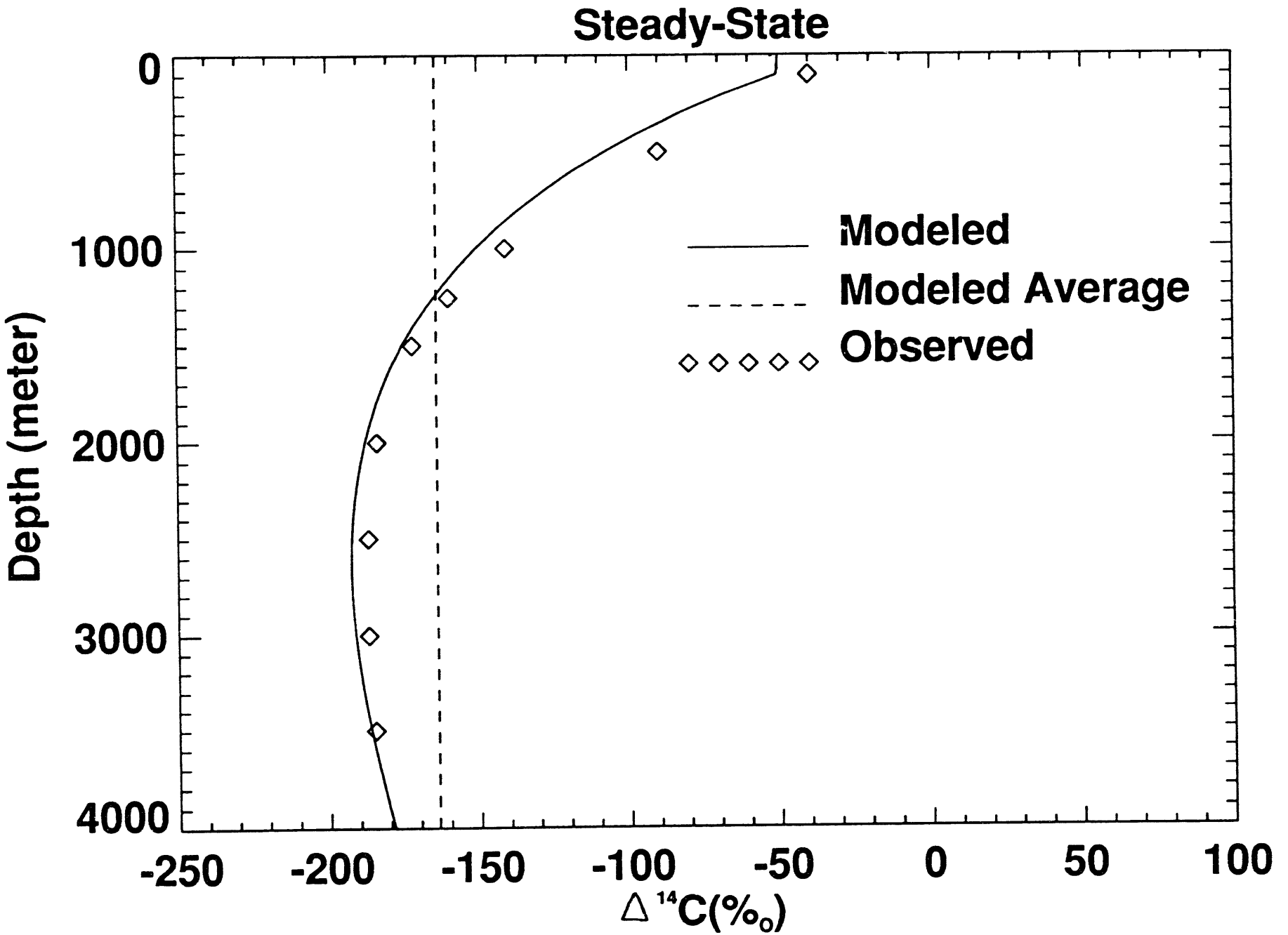
Steady-State
0
1000
2000
3000
4000
Depth (meter)
Modeled
Modeled Average
Observed
-250
-200
-150
-100
-50
0
50
100
Δ 14C(‰)

Figure 8

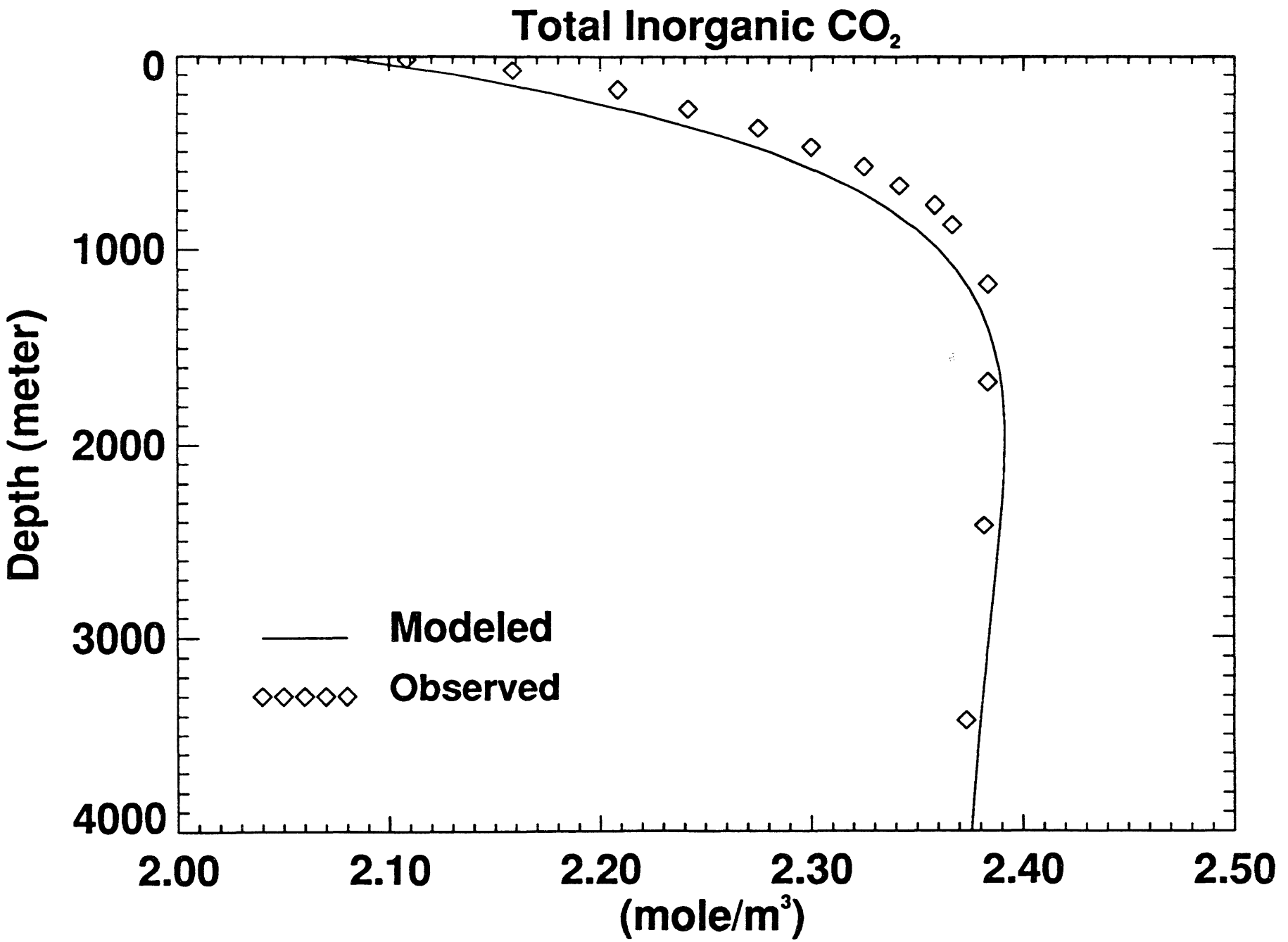
Total Inorganic CO_2
0
1000
2000
3000
4000
Depth (meter)
Modeled
Observed
2.00
2.10
2.20
2.30
2.40
2.50
(mole/m^3)

Figure 9

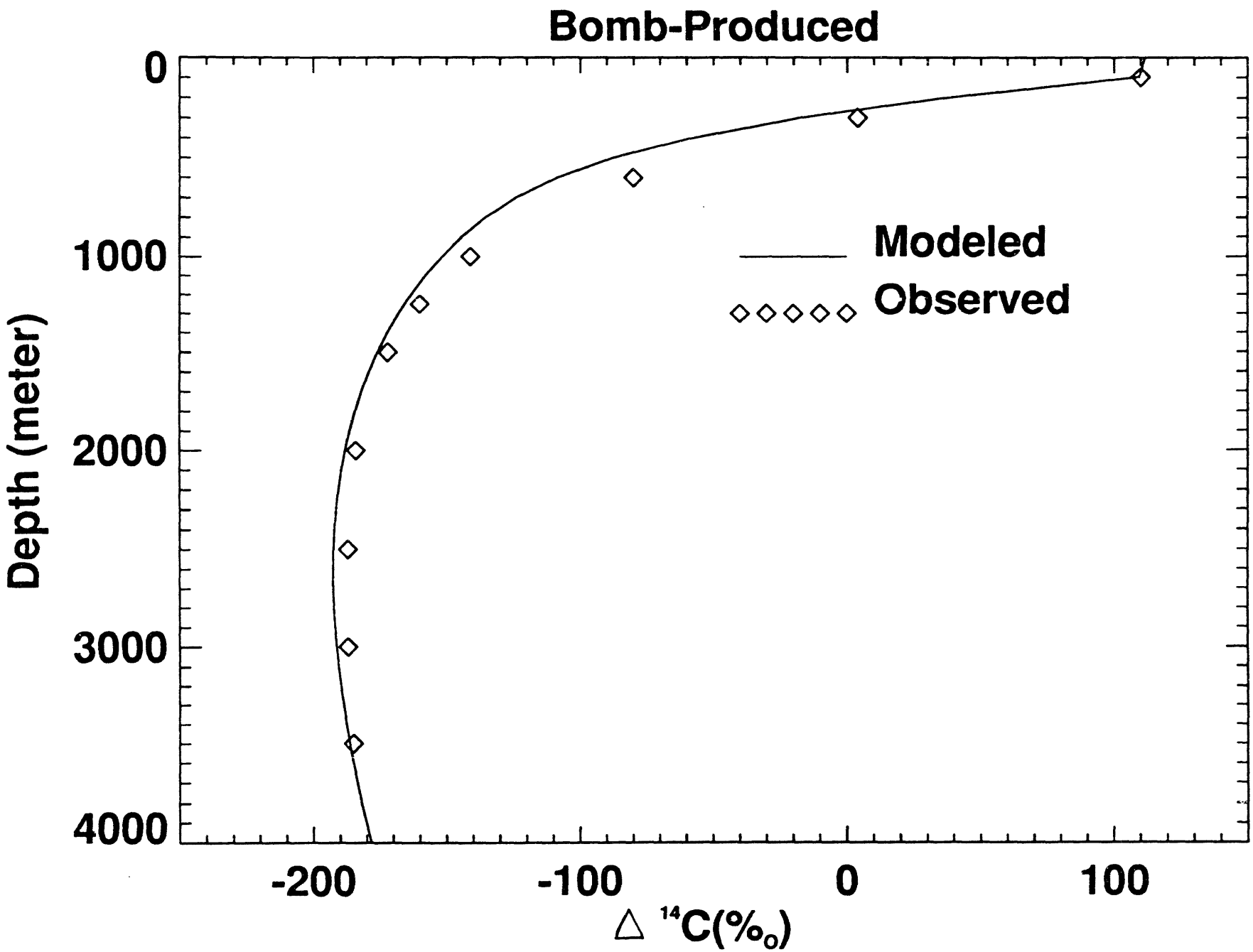
Bomb-Produced
0
1000
2000
3000
4000
Depth (meter)
Modeled
Observed
-200
-100
0
100
Δ ¹⁴C(‰)

Figure 10

DATE
FILMED
4 / 15 / 94
END